

Original Paper

Vasopressin Neurons Respond to Hyperosmotic Stimulation with Regulatory Volume Increase and Secretory Volume Decrease by Activating Ion Transporters and Ca²⁺ Channels

Kaori Sato-Numata^{a,b} Tomohiro Numata^b Yoichi Ueta^c Yasunobu Okada^{d,e,f}

^aJapan Society for the Promotion of Science, Tokyo, Japan, ^bDepartment of Physiology, School of Medicine, Fukuoka University, Fukuoka, Japan, ^cDepartment of Physiology, School of Medicine, University of Occupational and Environmental Health, Fukuoka, Japan, ^dNational Institute for Physiological Sciences, Okazaki, Japan, ^eDepartment of Physiology, School of Medicine, Aichi Medical University, Nagakute, Japan, ^fDepartment of Physiology, Kyoto Prefectural University of Medicine, Kyoto, Japan

Key Words

Vasopressin neuron • Regulatory volume increase • Secretory volume decrease • Calcium channel • Hyperosmotic stimulation

Abstract

Background/Aims: Arginine vasopressin (AVP) neurons play an important role for sensing a change in the plasma osmolarity and thereby responding with regulated AVP secretion in order to maintain the body fluid homeostasis. The osmo-sensing processes in magnocellular neurosecretory cells (MNCs) including AVP and oxytocin (OXT) neurons of the hypothalamus were reported to be coupled to sustained osmotic shrinkage or swelling without exhibiting discernible cell volume regulation. Since increasing evidence has shown some important differences in properties between AVP and OXT neurons, osmotic volume responses are to be reexamined with distinguishing these cell types from each other. We previously reported that AVP neurons identified by transgenic expression of enhanced green fluorescence protein (eGFP) possess the ability of regulatory volume decrease (RVD) after hypoosmotic cell swelling. Thus, in the present study, we examined the ability of regulatory volume increase (RVI) after hyperosmotic cell shrinkage in AVP neurons. **Methods:** Here, we used eGFP-identified AVP neurons acutely dissociated from AVP-eGFP transgenic rats. We performed single-cell size measurements, cytosolic RT-PCR analysis, AVP secretion measurements, and patch-clamp studies. **Results:** The AVP neurons were found to respond to a hyperosmotic challenge with physiological cell shrinkage caused by massive secretion of AVP, called a secretory

volume decrease (SVD), superimposed onto physical osmotic cell shrinkage, and also to exhibit the ability of RVI coping with osmotic and secretory cell shrinkage. Furthermore, our pharmacological and molecular examinations indicated that AVP secretion and its associated SVD event are triggered by activation of T-type Ca^{2+} channels, and the RVI event is attained by parallel operation of Na^+/H^+ exchanger and $\text{Cl}^-/\text{HCO}_3^-$ anion exchanger. **Conclusion:** Thus, it is concluded that AVP neurons respond to hyperosmotic stimulation with the regulatory volume increase and the secretory volume increase by activating ion transporters and Ca^{2+} channels, respectively.

© 2021 The Author(s). Published by
Cell Physiol Biochem Press GmbH&Co. KG

Introduction

Arginine vasopressin (AVP) is an antidiuretic hormone which maintains osmotic pressure stability in the body fluid. AVP-producing neurons are localized in the supraoptic nucleus (SON) and paraventricular nucleus (PVN) of the hypothalamus. Synthesized AVP in these AVP neurons is secreted by an exocytotic mechanism into the systemic circulation from the axon terminal extending to the posterior pituitary gland. The amount of AVP secreted into the systemic circulation is controlled in the hypothalamus by osmo-sensing information derived not only from the axons of osmosensory neurons localized in the organum vasculosum laminae terminalis (OVLT) and subfornical organ (SFO) but also directly from AVP neurons themselves in the SON and PVN.

Cell volume regulation is, in general, a prerequisite function coping with osmotic perturbation in animal cells to survive under both physiological and pathological conditions [1-5]. In contrast, the osmo-sensing processes in magnocellular neurosecretory cells (MNCs), which consist of AVP neurons and oxytocin (OXT) neurons, were, in particular, reported to be coupled to sustained osmotic shrinkage or swelling without exhibiting discernible cell volume regulation [6]. In rat AVP neurons distinguished from OXT neurons by transgenic expression of enhanced green fluorescence protein (eGFP), on the other hand, we recently found that an acute hypoosmotic challenge induces rapid osmotic cell swelling followed by slow cell volume regulation, called the regulatory volume decrease (RVD) which is essentially mediated by activation of volume-sensitive outwardly rectifying anion channel (VSOR) [7]. However, it remains to be examined whether the eGFP-identified AVP neurons can respond to acute hyperosmotic stress with the regulatory volume increase (RVI) after osmotic shrinkage.

AVP neurons secrete AVP not only from the axon terminal to regulate the body fluid homeostasis but also from the soma and dendrites within the brain [8-11] to exert a variety of autocrine/paracrine actions, such as depressing effects on the EPSCs in MNCs [12], optimizing effects on the phasic firing pattern of the neurons [13], promoting effects on the reconstitution of local arterioles within the hypothalamic nuclei [14], and facilitating effects on their RVD process by augmenting VSOR activity [7]. Both axonal terminal secretion and somato-dendritic release of AVP and OXT from MNCs are known to be sensitive to tetanus toxin (TeTx) [8, 15] and dependent on Ca^{2+} [8, 11, 15-19], indicating an involvement of exocytotic secretory mechanism. Sustained cell shrinkage, called a secretory volume decrease (SVD) [20], was observed in a number of secretory cells under stimulation with secretagogues until the stimuli are withdrawn [5, 20-27]. Thus, there is a possibility that such an SVD event is coupled to somato-dendritic AVP release from dissociated AVP neurons in response to a hyperosmotic challenge.

In the present study, we examined whether AVP neurons exhibit, in addition to osmotic cell shrinkage, SVD and RVI in response to acute hyperosmotic stimulation, by using AVP neurons isolated from transgenic rats expressing eGFP under the control of the AVP promoter [28] in the single-cell preparation free of OXT neurons, glia cells, and connective tissue cells. Our data indicated that AVP neurons respond to a hyperosmotic challenge not only with physical osmotic shrinkage but also a physiological SVD event, which is sensitive to TeTx and blockers for T-type calcium channels, and also do possess the RVI ability, which is sensitive to blockers for Na^+/H^+ exchanger (NHE) and $\text{Cl}^-/\text{HCO}_3^-$ anion exchanger (AE).

Materials and Methods

Animals and Preparation of Acutely Dissociated AVP Neurons

All procedures involving animals were approved in advance by the Ethics Review Committee for Animal Experimentation of Fukuoka University and were in accordance with the guidelines of the Physiological Society of Japan. Non-transgenic female Wistar rats (Charles River Laboratories Japan, Yokohama, Japan) and heterozygous transgenic female Wistar rats, which express an AVP-enhanced green fluorescent protein (eGFP) fusion gene [28], were bred and housed under standardized conditions (12-h:12-h light/dark cycle) with food and water. For all the experiments, 4–5-week old AVP-eGFP transgenic female rats were used.

Acutely dissociated AVP neurons were prepared, as described previously [7], and incubated in Ringer solution containing (in mM): 140 NaCl, 5 KCl, 1 MgCl₂, 2 CaCl₂, 10 HEPES and 10 glucose (adjusted to pH 7.25 with Tris, 300 mosmol/kg-H₂O, bubbled with 100% O₂) at room temperature (22–26°C). In all of the experiments, eGFP expression was confirmed each time under a fluorescence microscope to identify given SON neurons as AVP neurons.

Single Cell Size Measurements

Single-cell size was measured at room temperature in AVP neurons adhered to a cover glass that were exposed to hyperosmotic solution (430 mosmol/kg-H₂O) after a 45-min preincubation with isoosmotic solution (315 mosmol/kg-H₂O). The experimental solutions contained (in mM): 120 NaCl, 2.5 KCl, 2 MgCl₂, 2 CaCl₂, 25 NaHCO₃, 10 glucose (315 or 430 mosmol/kg-H₂O adjusted with mannitol). Solutions were always prepared immediately before experimental use to achieve reproducible HCO₃ concentrations and bubbling with 5% CO₂ throughout the experiments. The cells were visualized with a charge-coupled device camera (ORCA-ER-1394, Hamamatsu Photonics) and recorded with AquaCosmos software (version 2.0: Hamamatsu Photonics). The CSA of the soma was measured as an indicator of cell size by ImageJ software. To inhibit exocytosis, we preincubated cells with isoosmotic solution containing 15 nM tetanus toxin (TeTx: Sigma-Aldrich, Tokyo, Japan) for 70 min, and then we performed experiments by applying hyperosmotic solution in the presence of TeTx.

RNA Isolation and RT-PCR

Using the RNeasy Micro Kit (Qiagen, Tokyo, Japan), total cellular RNAs were extracted from the cytosol suctioned into patch pipettes from 10 AVP neurons and pooled. RNA samples were reverse-transcribed using the ReverTra Ace qPCR RT Master Mix (TOYOBO, Osaka, Japan) according to the manufacturer's protocols. Gene-specific primers used for PCR were designed with Primer3 software (<http://frodo.wi.mit.edu/primer3/>) and NCBI BLAST (<http://blast.ncbi.nlm.nih.gov/Blast.cgi>) to identify complementary sequences in the rat genome. The primers sequences used in the RT-PCR experiments were listed in Table 1 along with the product sizes and GenBank accession numbers. As a positive control, we amplified the glyceraldehyde-3-phosphate-dehydrogenase (GAPDH) sequence. As a negative control, we performed RT-PCR without reverse transcriptase. PCR was performed with 0.4 U of KOD -Plus- Neo Taq (TOYOBO). Amplification was carried out in a thermal cycler (Tadvanced 96 SG: Biometra, Göttingen, Germany) under the following conditions: initial heating at 94°C for 2.5 min, followed by 40 cycles of denaturation at 94°C for 15 s, annealing at 60°C for 30 s and extension at 68°C for 1 min, and then final extension at 68°C for 5 min. The products of RT-PCR were electrophoresed on a 2% agarose gel, and then cloned into the pGEM-T Easy vector (Promega, Tokyo, Japan) after purification with the Wizard SV Gel and PCR Clean-Up System (Promega). Plasmids were purified with the Wizard Plus Minipreps DNA Purification System (Promega) and used as templates for sequencing with ABI PRISM 310 genetic analyzer (Applied Biosystems, Foster City, CA) or with ABI 3730xl genetic analyzer (FASMAC, Kanagawa, Japan)

Measurements of AVP Secretion

The amounts of AVP secretion from dissociated AVP neurons exposed to isoosmotic and hyperosmotic solutions were measured at 37°C using the arg⁸-Vasopressin Enzyme Immunoassay Kit (Assay Designs, Ann Arbor, MI) according to the manufacturer's protocol. The experimental solutions were the same as used in the single cell size measurements. After a 20-min preincubation of a batch of ~3800 isolated neurons in 200 mL of iso-osmotic solution, 800 mL of isoosmotic or hyperosmotic solution was added to the cell suspension and the cells were incubated for 90 min. These solutions were then centrifuged at 400g for 10 min at 4°C.

Table 1. Primer sequences used in RT-PCR analyses for rat NHEs, AEs, ENaCs, TRPM2 and GAPDH

Genes	GenBank accession no.	Forward primer sequence (5'→3')	Reverse primer sequence (5'→3')	PCR product
<i>NHE1</i>	NM_012652.1	GAGCTCTTCCACCTGTCTGG	AAGGTGGTCCAGGAAGTGTG	555 bp
<i>NHE2</i>	NM_001113335.1 NM_012653.2	AGGAAGGCAGAGGAAGGAAG	AAAGCCATGGAACACACAGG	523 bp
<i>NHE3</i>	NM_012654.1	GGAAGAGAGCTGGGAGGAGT	CGGCTGCTAGCTTTGGTATC	498 bp
<i>NHE4</i>	NM_173098.1	GGTGTGAGAGGAGCAGGAAG	TAGCCAGTCTCTGCCATCT	408 bp
<i>NHE5</i>	NM_138858.1	GTGTCCCACATCTTGCTTT	CCAACCTGAAACCTTGAGA	415 bp
<i>AE1</i>	NM_012651.2	CCCAACTTGTACGAGGCATT	CCAGCAGGATAAGCCAGAAG	451 bp
<i>AE2</i>	NM_017048.2	GAGCCCTTCTGCTGAAACAC	GGCATTGATAGCAGTCAGCA	551 bp
<i>AE3</i>	NM_017049.1	CAGGGCTCTCAGTGACTTCC	ACGCTGGGACAAGTGGATAC	518 bp
<i>α-ENaC</i>	NM_031548.2	GTCCCAGGATTGGATCTTCGAG	ATCAGTTTACAAGGAGCTCAGG	576 bp
<i>β-ENaC</i>	NM_012648.1	CACTCCACCTCCCAACTATGAC	AAGCCTTCTTACCTGATGCTCC	463 bp
<i>γ-ENaC</i>	NM_017046.1	GAGTCGAAGAACTGGTGGGAT	AAGTGGACATTGCTGTCTCGAT	472 bp
<i>TRPM2</i>	NM_001011559.1	TTTGCTACGTGCTCATGGT	TTCACGCCGTCAATGTAGGT	533 bp
<i>GAPDH</i>	NM_017008.3	CATGCCGCTGGAGAACTGCCA	GGGCTCCCAGGCCCTCTCTGT	429 bp

Extraction of AVP was performed with the supernatants, which were applied onto C-18 SEP-COLUMNS (Phoenix Pharmaceuticals, Burlingame, CA) according to the manufacturer's protocol using buffers A and B (Phoenix Pharmaceuticals). Extracted AVP was dried with a vacuum freeze-dryer (VD-800F; Taitec). AVP was assayed with a Microplate reader (MultiscanMS-UV, Lab Systems) at a wavelength of 414 nm. To inhibit exocytosis, we preincubated cells in isoosmotic solution containing 15 nM TeTx for 70 min, and then we performed experiments by applying hyperosmotic solution containing TeTx.

Electrophysiology

The patch electrodes had a resistance of around 1–3 MΩ. Currents or voltages were recorded using an Axopatch 200B amplifier (Axon Instruments, Union City, CA) coupled to DigiData 1440A A/D and D/A converters (Axon Instruments). Currents or voltage signals were filtered at 5 kHz and digitized at 20 kHz. pClamp software (version 9.0.2; Axon Instruments) was used for command pulse control, data acquisition and analysis. For the measurements of Ca²⁺ channel currents, whole-cell voltage-clamp recordings were performed at room temperature. The time course of current activation was monitored by repetitively applying (every 10 s) alternating pulses (0.3-s duration) of –10 mV from a holding potential of –80 mV. To observe voltage dependence of the current profile, step pulses were applied (every 10 s) from the holding potential to test potentials of –60 mV to +70 mV for 0.3 s in 10 mV increments. For the peak value, we measured the largest value among the inward currents observed immediately after stimulation of the test pulse. For the steady-state value, we measured the value at 280 ms after stimulation of the test pulse. Series resistance (<10 MΩ) was compensated (to 70–80%) to minimize voltage errors. The intracellular (pipette) solution contained (in mM): 160 NMDG-phosphate, 4 MgCl₂, 40 HEPES, 10 EGTA, 12 phosphocreatine, 0.1 leupeptine, 2 ATP-Tris salt and 0.4 GTP-Tris salt (280 mosmol/kg-H₂O, adjusted to pH 7.2 with phosphoric acid). The isoosmotic or hyperosmotic extracellular (bath) solution (300 or 380 mosmol/kg-H₂O) contained (in mM): 60 TEA-Cl, 10 HEPES, 50 BaCl₂, 10 glucose and 0 or 80 mannitol (adjusted to pH 7.3 with TEA-OH). For the measurements of membrane potential and spontaneous firing, perforated whole-cell current-clamp recordings were performed at 32–35°C controlled by using an automatic temperature controller (TC-324; Warner Instruments, Hamden, CT) with the pipette solution containing (in mM): 99 K₂SO₄, 31 KCl, 5 MgCl₂, 0.2 EGTA, 5 HEPES (280 mosmol/kg-H₂O, adjusted to pH 7.4 with KOH). Pipette solution was placed in the tip of the pipette by capillary action (~5 s), and then pipettes were backfilled with nystatin-containing (200 μg/mL) pipette solution. The isoosmotic or hyperosmotic bath solution (300 or 380 mosmol/kg-H₂O) contained (in mM): 120 NaCl, 5 KCl, 2 CaCl₂, 1 MgCl₂, 10 glucose, 10 HEPES and 20 or 100 mannitol (adjusted to pH 7.3 with NaOH).

Statistical Analysis

Data are given as the means \pm SEM of observations (n). Statistical differences of the data were evaluated using one-way ANOVA followed by a Bonferroni-type for multiple comparisons and considered to be significant at $p < 0.05$.

Chemicals

All chemicals except nickel were prepared on the day of the experiments by diluting stock solutions of 1000-fold concentrations. Ni^{2+} (Wako Pure Chemical) was directly made in the solution for each experiment and used during that day. The stocks of flufenamic acid (FFA: Sigma-Aldrich), 4,4'-diisothiocyanatostilbene-2,2'-disulfonic acid disodium salt hydrate (DIDS; Sigma-Aldrich), benzamil (Sigma-Aldrich), and 3-aminobenzamide (3-AB: Sigma-Aldrich) were made in dimethyl sulfoxide (DMSO: Wako Pure Chemical, Osaka, Japan) and kept at -20°C . The stocks of TeTx, ω -conotoxin GVIA (ω -CgTx: PEPTIDE INSTITUTE, INC., Osaka, Japan), and amiloride (Sigma-Aldrich) were made in distilled water and kept at -20°C .

Results

Persistent Osmotic Shrinkage in Dissociated AVP Neurons under Hyperosmotic Stimulation and Its Aggravation by Blocking the NHE and AE Activities

When dissociated AVP neurons were exposed to hyperosmotic extracellular solution (136.5% osmolarity), the cross-sectional area (CSA) of AVP neurons became rapidly smaller, and such hyperosmotic cell shrinkage persisted over 90 min, as shown in Fig. 1 (a: open squares; b: Control), being consistent with a previous report for MNCs [6]. Since AVP neurons apparently lack the RVI ability, we next examined molecular expression of NHE and AE transporters as well as of the epithelial Na^{+} channel (ENaC) and the transient receptor potential cation channel, subfamily M, member 2 (TRPM2), that are both known to be responsible for the hypertonicity-induced cation channel (HICC) [29, 30], in AVP neurons, because the volume-regulatory NaCl influx involved in the RVI event is known to be attained by these Na^{+} and Cl^{-} transporters or Na^{+} -permeable cation channels in a variety of animal cells [29, 31-33]. As shown in Fig. 2a, cytosol RT-PCR analysis showed significant expression of mRNAs for NHE1, NHE4, NHE5, AE2, AE3, and TRPM2 in AVP neurons. The sequences of above six transporter/channel genes expressed in AVP neurons were found to completely match by sequence analysis to the sequences corresponding to their respective rat NHEs, AEs and TRPM2. On the other hand, any ENaC mRNAs were not detected in the cytosol of AVP neurons (Fig. 2a), although α -, β -, and γ -ENaC were all sizably detected in the SON region (Fig. 2b). The sequences of above three ENaC genes expressed in the SON region completely matched to the sequences corresponding to their respective rat ENaC channels. Thus, the effects of blockers for these transporters and channels on hyperosmotic cell shrinkage were next examined by measuring the CSA of AVP neurons. When applying an NHE blocker, amiloride (100 μM), or an AE blocker, DIDS (100 μM), osmotic cell shrinkage became prominently exaggerated, as shown in Fig. 1a (filled symbols). In the presence of amiloride or DIDS, as summarized in Fig. 1b (+amiloride/+DIDS), the shrinking CSA change never recovered even after 90 min after a hyperosmotic challenge and moreover became much more shrunken by around 30%. In contrast, applications of an ENaC blocker, benzamil [34], and a blocker of poly (ADP-ribose) polymerase (PARP), 3-AB [35], which thereby inhibits PARP-dependent TRPM2 channel activity [36], failed to affect the persistent cell shrinkage even 90 min after a hyperosmotic challenge (Fig. 1b). These results suggest that AVP neurons do possess the RVI ability, in which NHE and AE are involved, though they apparently exhibit sustained shrinkage under hyperosmotic stimulation.

Fig. 1. The effects of blockers for NHE, AE, ENaC and PARP on osmotic shrinkage induced by hyperosmotic stimulation in AVP neurons. (a) Time course of changes in the cross-sectional area (CSA) of the cell soma before and after application of hyperosmotic bath solution (at arrow) in the absence (Control) or presence of an NHE blocker, amiloride (100 μ M), or an AE blocker, DIDS (100 μ M). (b) Percentage of recovery of CSA (from Control peak osmotic shrinkage) at 90 min after application of hyperosmotic bath solution in the absence (Control) or presence of amiloride (100 μ M), DIDS (100 μ M), benzamil (10 μ M), or 3-AB (300 μ M). * p <0.05 vs. Control (n=12-33).

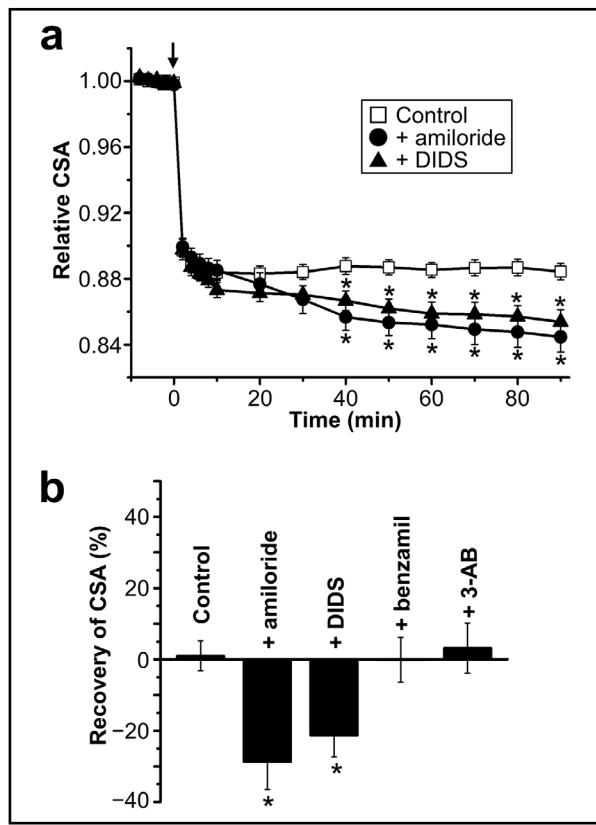
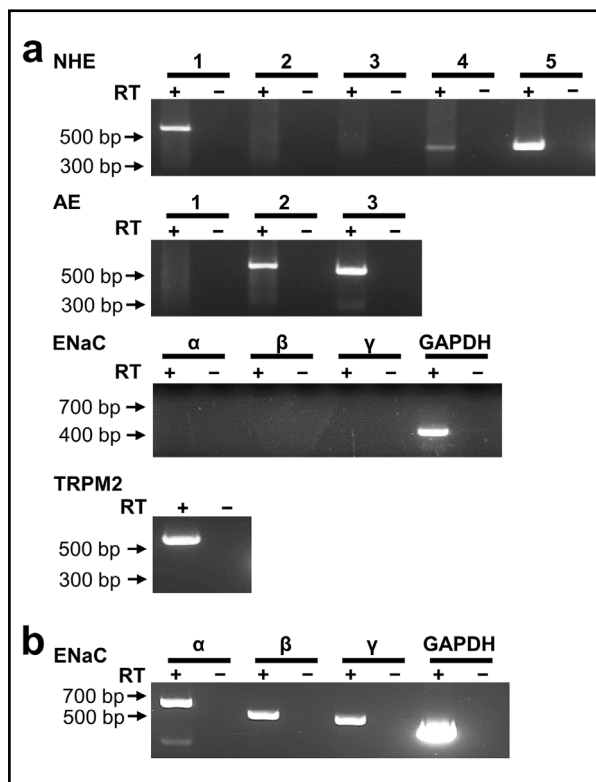


Fig. 2. Molecular expression of Na⁺ and Cl⁻ transporters and Na⁺-permeable cation channels detected by RT-PCR in AVP neurons and the SON region. (a) Expression of mRNAs encoding NHE, AE, ENaC, and TRPM2 in AVP neurons. The pooled cytosol of 10 AVP neurons was used in RT-PCR for *NHE1* (555base pairs (bp)), *NHE2* (523 bp), *NHE3* (498 bp), *NHE4* (408 bp), *NHE5* (415 bp), *AE1* (451 bp), *AE2* (551 bp), *AE3* (518 bp), α -*ENaC* (576 bp), β -*ENaC* (463 bp), γ -*ENaC* (472 bp), *TRPM2* (533 bp), or *GAPDH* (429 bp) (n=4-10). Sequence analyses showed that the above seven genes sizably detected in AVP neurons were completely matched to the sequences corresponding to their respective rat *NHE1*, *NHE4*, *NHE5*, *AE2*, *AE3*, *TRPM2*, and *GAPDH*. (b) Expression of mRNAs encoding ENaC in the SON region. The block of SON region was used in RT-PCR for rat α -*ENaC*, β -*ENaC*, γ -*ENaC*, and *GAPDH* (n=4). The above four genes expressed in the SON region were completely matched to the sequences corresponding to their respective mRNAs. RT (+) and RT (-) represent lanes with and without reverse transcriptase.



Prominent RVI Event Sensitive to Blockers of NHE and AE in Dissociated AVP Neurons under the Conditions where Hyperosmolarity-Induced AVP Secretion was Inhibited

When AVP neurons were exposed to hyperosmotic solution containing flufenamic acid (FFA, 100 μ M), which was shown to markedly suppress T- and N-type voltage-gated Ca^{2+} channel (VGCC) currents and thereby abolish action potential firings in AVP neurons under isotonic conditions [37], the RVI event surprisingly became evident (Fig. 3a: filled circles) in a manner sensitive to amiloride and DIDS at 100 μ M (Fig. 3a: filled triangles and reversed triangles). A similar prominent RVI event was also observed in the presence of a blocker of vesicular exocytotic secretion, TeTx (15 nM), or a known blocker of VGCC, Ni^{2+} (3 mM), which was found to predominantly suppress T-type VGCC currents and thereby abolish action potential firings in AVP neurons under normotonic conditions [37], in dissociated AVP neurons under hyperosmotic conditions (Fig. 3b). As summarized in Fig. 3c, TeTx, Ni^{2+} and FFA recovered the CSA by 50 to 60% in dissociated AVP neurons 90 min after a hyperosmotic challenge, and the FFA-induced CSA recovery was abolished by amiloride and DIDS. Since release of AVP and OXT from MNCs are known to be inhibited by TeTx [8, 15] and to be dependent on Ca^{2+} influx through VGCCs [38-41], it is likely that the FFA effects on the CSA changes in AVP neurons after a hyperosmotic challenge are caused by inhibiting hyperosmotic AVP secretion. In fact, hyperosmolarity-induced AVP secretion was remarkably inhibited not only by TeTx and Ni^{2+} but also by FFA, as shown in Fig. 3d. These results indicate that AVP neurons respond to hyperosmotic stimulation with the SVD event caused by massive vesicular exocytotic release of AVP, superimposed onto osmotic cell shrinkage. It is noted that they exhibited the NHE- and AE-dependent RVI event in opposition to such dual volume-decreasing events.

Sensitivity of Action Potential Firing Activity to FFA and Ni^{2+} in Dissociated AVP Neurons under Hyperosmotic Stimulation

It is known that AVP secretion depends on action potential firing activity which stimulates Ca^{2+} entry via VGCCs in MNCs [42-46]. Also, we recently found that FFA and Ni^{2+} abolish action potential firings in rat AVP neurons under normotonic conditions [37]. Thus, we examined the effects of FFA and a known VGCC blocker, Ni^{2+} , on the firing activity in dissociated AVP neurons after hyperosmotic stimulation by nystatin-perforated whole-cell current-clamp recordings. When the neurons were exposed to a hyperosmotic solution (126.7% osmolarity), the firing activity was markedly enhanced with inducing a slight depolarizing shift of the resting membrane potential, as shown in Fig. 4. These results are in good agreement with previous observations [45, 47-49]. The firing activity observed after hyperosmotic stimulation was prominently suppressed by application of FFA (Fig. 4a) and Ni^{2+} (Fig. 4b). The firing frequency was increased around three-fold by hyperosmotic stimulation and was almost completely abolished by application of FFA and Ni^{2+} (Fig. 4c). In contrast, hypertonicity-enhanced action potential firing activity in AVP neurons were, as shown in Fig. 4c, not affected by application of ω -CgTx (0.5 μ M), which is a specific blocker of N-type Ca^{2+} channels [50-52] and was found to predominantly suppress N-type VGCC currents in AVP neurons under isotonic conditions [37]. These results suggest that FFA inhibits hyperosmolarity-induced AVP secretion and thereby the SVD event by inhibiting the firing activity presumably through suppression of Ni^{2+} -sensitive T-type VGCCs in AVP neurons under hyperosmotic conditions.

Sensitivity of the Ca^{2+} Channel Activities to FFA and Ni^{2+} in Dissociated AVP Neurons under Hyperosmotic Stimulation

To examine whether FFA and Ni^{2+} actually suppresses VGCC currents in dissociated AVP neurons under not only isotonic but also hyperosmotic conditions, we then made conventional whole-cell recordings. Under exposure to 50 mM Ba^{2+} , AVP neurons showed Ba^{2+} currents through VGCCs exhibiting the peak inward currents at around -10 mV under

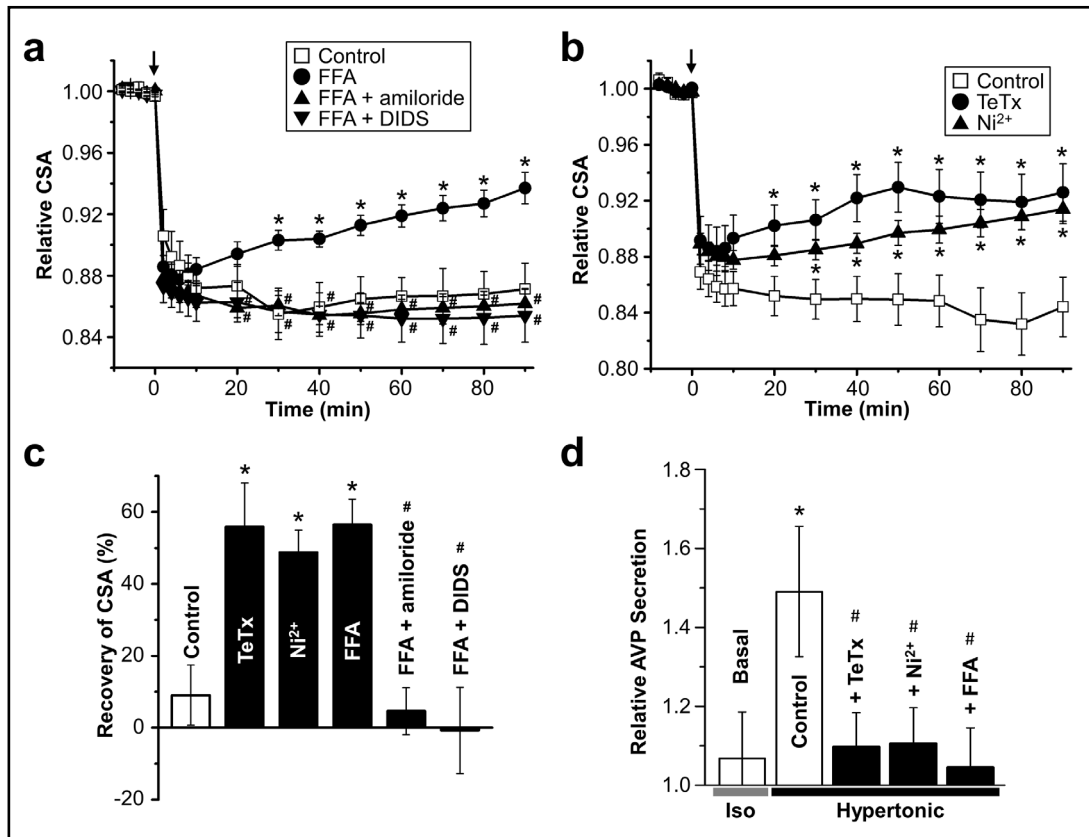


Fig. 3. The effects of FFA, TeTx and Ni²⁺ on osmotic shrinkage in and AVP secretion from AVP neurons in response to hyperosmotic stimulation. (a) Time course of changes in the cross-sectional area (CSA) of the cell soma before and after application of hyperosmotic bath solution (at arrow) in the absence (Control) or presence of FFA (100 μM), FFA plus amiloride (100 μM) or FFA plus DIDS (100 μM) (n=11-19). (b) Time course of changes in the cross-sectional area (CSA) of the cell soma before and after application of hyperosmotic bath solution (at arrow) in the absence (Control) or presence of TeTx (15 nM) or Ni²⁺ (3 mM) (n=8-14). TeTx was applied for 70 min before hyperosmotic stimulation as well. (c) Percent recovery of CSA (from the average of Control peak osmotic shrinking) at 90 min after a hyperosmotic challenge in the absence or presence of drugs (n = 9-19). *p<0.05 vs. Control. #p<0.05 vs. in the presence of FFA. (d) The relative amount of AVP released from dissociated SON neurons for 90 min after application of isosmotic (Basal; n=16) or hyperosmotic bath solution in the absence (Control) or presence of TeTx, Ni²⁺, or FFA (n=7-21). *p<0.05 vs. Basal. #p<0.05 vs. Control.

isotonic conditions (Fig. 5a: Iso), as observed in our recent studies under normotonic conditions [37]. A hyperosmotic challenge (126.7% osmolality) did not significantly affect depolarization-induced Ba²⁺ currents (Fig. 5a: Hyper), indicating that the VGCCs in AVP neurons *per se* do not exhibit osmosensitivity. As found in our preceding study [37], VGCC currents in AVP neurons under normotonic conditions were largely suppressed by Ni²⁺ (3 mM) with shifting the voltage showing the peak current from around -10 mV to around +10 mV (Fig. 5b), whereas they were suppressed by ω-CgTx (0.5 μM) without shifting the voltage showing the peak current (Fig. 5c). Ni²⁺-insensitive currents observed under isosmotic conditions, which were shown to represent mainly N-type VGCC currents [37], were little affected by a hyperosmotic challenge (Fig. 5b). The Ni²⁺-insensitive current observed under hyperosmotic conditions was markedly suppressed by ω-CgTx (Fig. 5b). Also, ω-CgTx-insensitive currents observed under isosmotic conditions, which was shown to represent mainly T-type VGCC currents [37], were also little affected by a hyperosmotic challenge (Fig. 5c). The ω-CgTx-insensitive current observed under hyperosmotic conditions

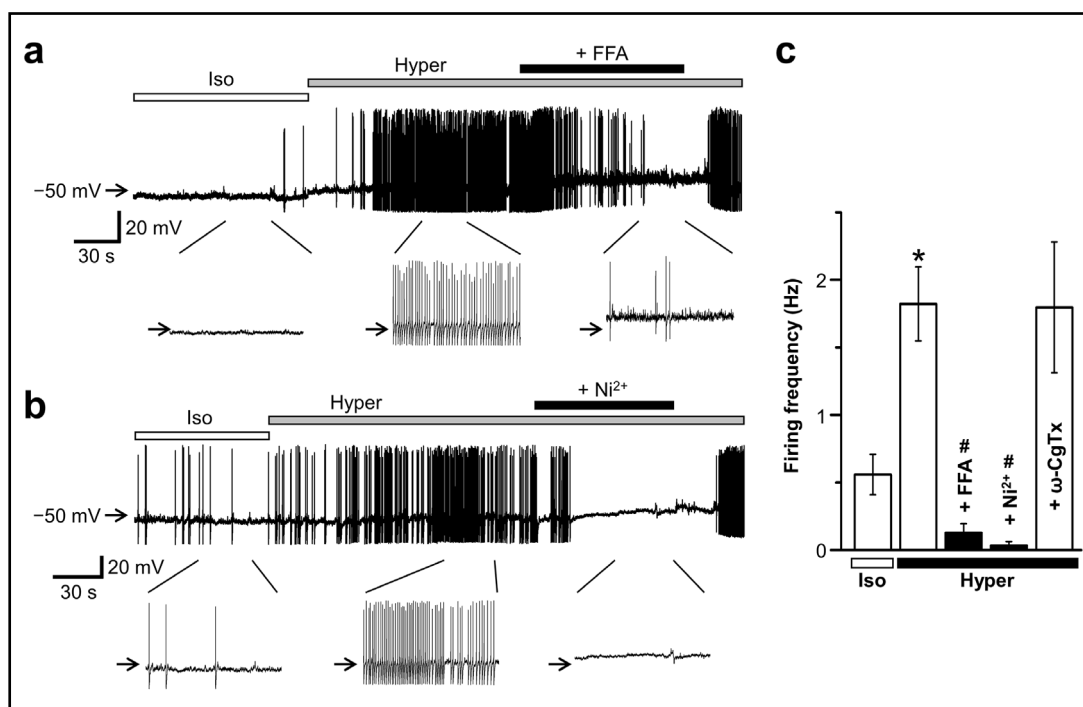


Fig. 4. The effects of hyperosmotic stimulation and application of FFA or Ni²⁺ on spontaneous action potential firings in AVP neurons. (a, b) Representative records of spontaneous action potential firings under isosmotic (Iso) or hyperosmotic (Hyper) conditions and before and after application of FFA (a: +FFA, n=8) or Ni²⁺ (b: +Ni²⁺, n=10). Insert panels given below the traces of membrane potential changes represent expanded traces for the indicated parts of the records for 30 s. Arrows represent the membrane potential level of -50 mV. (c) The averages of the firing frequency (Hz) under isosmotic (Iso) or hyperosmotic (Hyper) conditions in the absence and presence of FFA, Ni²⁺ or ω-CgTx (n=8-27). *p<0.05 vs. Iso. #p<0.05 vs. Hyper in the absence of blockers.

was mostly abolished by Ni²⁺ (Fig. 5c). These results indicate that VGCC currents observed in AVP neurons under hyperosmotic conditions are composed mainly of T-type and N-type Ca²⁺ channels, as was the case of those observed under isosmotic conditions [37].

When FFA was applied to AVP neurons, their VGCC currents observed under hyperosmotic conditions were markedly suppressed by FFA (Fig. 6a, d), just as the case of those observed under isotonic conditions [37]. In the presence of ω-CgTx, FFA suppressed the remaining (mainly T-type) VGCC currents (Fig. 6b, d); and also, in the presence of Ni²⁺, FFA largely diminished the remaining (mainly N-type) VGCC currents (Fig. 6c, d) in AVP neurons under hyperosmotic conditions. Taken together, it is concluded that FFA and Ni²⁺ block voltage-gated Ca²⁺ channel activities in dissociated rat AVP neurons under hyperosmotic conditions and thereby inhibit the SVD event coupled to hypertonicity-induced AVP secretion.

Discussion

Release of AVP and OXT from MNCs in the hypothalamus is evoked by Ca²⁺ influx through VGCCs [41, 53, 54]. Previous electrophysiological studies on VGCC currents showed that the soma of rat SON MNCs express T-, N-, L-, P/Q- and R-type Ca²⁺ channels [55-59]. Among these types of VGCCs, somato-dendritic expression of T-, N- and L-type Ca²⁺ channels in AVP neurons were indirectly suggested by observing sensitivity to VGCC blockers of increases in [Ca²⁺]_i in response to AVP [46] and pituitary adenylate cyclase-activating polypeptide (PACAP) [60]. Although direct electrophysiological studies showed expression of L-, N- and

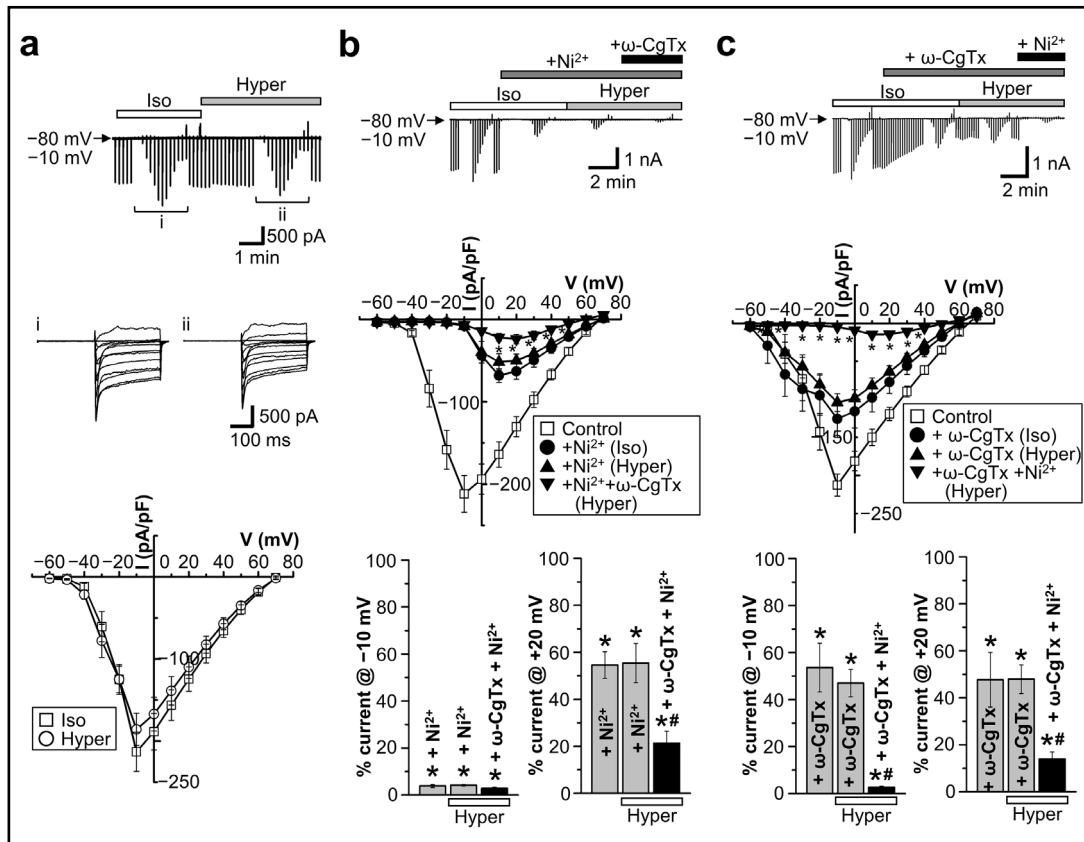


Fig. 5. The effects of Ni^{2+} and $\omega\text{-CgTx}$ on VGCC currents under isosmotic (Iso) or hyperosmotic (Hyper) conditions. (a) Representative record of currents before and after application of hyperosmotic bath solution (upper) and I-V relationships (bottom; $n=14$). Inset panels (middle) represent the expanded traces of current responses to step pulses from -60 to $+70$ mV applied at i and ii. (b) Representative record of currents (upper), I-V relationships (middle) and percent currents observed at -10 mV (bottom, left panel) and $+20$ mV (bottom, right panel) in the presence of Ni^{2+} ($+\text{Ni}^{2+}$) under isosmotic and hyperosmotic conditions, and in the presence of Ni^{2+} plus $\omega\text{-CgTx}$ ($+\text{Ni}^{2+}+\omega\text{-CgTx}$) under hyperosmotic conditions (bottom; $n=6$). $*p<0.05$ between $+\text{Ni}^{2+}$ and $+\text{Ni}^{2+}+\omega\text{-CgTx}$ under hyperosmotic conditions in the middle panel and vs. Control in the bottom panel. $\#p<0.05$ vs. $+\text{Ni}^{2+}$ under hyperosmotic conditions in bottom panel. (c) Representative record of currents (upper), I-V relationships (middle) and percent currents observed at -10 mV (bottom, left panel) and $+20$ mV (bottom, right panel) in the presence of $\omega\text{-CgTx}$ ($+\omega\text{-CgTx}$) under isosmotic and hyperosmotic conditions, and $\omega\text{-CgTx}$ plus Ni^{2+} ($+\omega\text{-CgTx}+\text{Ni}^{2+}$) under hyperosmotic conditions (bottom; $n=8$). $*p<0.05$ between $+\omega\text{-CgTx}$ and $+\omega\text{-CgTx}+\text{Ni}^{2+}$ under hyperosmotic conditions in the middle panel and vs. Control in the bottom panel. $\#p<0.05$ vs. $+\omega\text{-CgTx}$ under hyperosmotic conditions in bottom panel.

P/Q-type of Ca^{2+} channels in the neurohypophysial nerve endings of rat AVP neurons under unstimulated normotonic conditions [39, 41], such studies have not been conducted in the soma/dendrites in AVP neurons. Under dehydration conditions, somato-dendritic L-type Ca^{2+} channel currents were found to be increased in both AVP and OXT neurons in rats after 16-24 h water deprivation [61], but such studies have not been done upon an acute hyperosmotic challenge. Also, T-type Ca^{2+} channel currents were recorded in guinea pig AVP-containing MNCs in the slice preparation of the SON under normotonic conditions [62]. Recently, we showed that in rat AVP neurons under normotonic conditions, T-type Cav3.1 and N-type Cav2.2 channels are molecularly and functionally expressed, but Cav3.1 is primary involved in their action potential generation [37]. In the present study, for the first time, expression of VGCCs was examined upon acute hyperosmotic stimulation in dissociated rat AVP neurons that are largely devoid of nerve terminals and were identified by transgenic

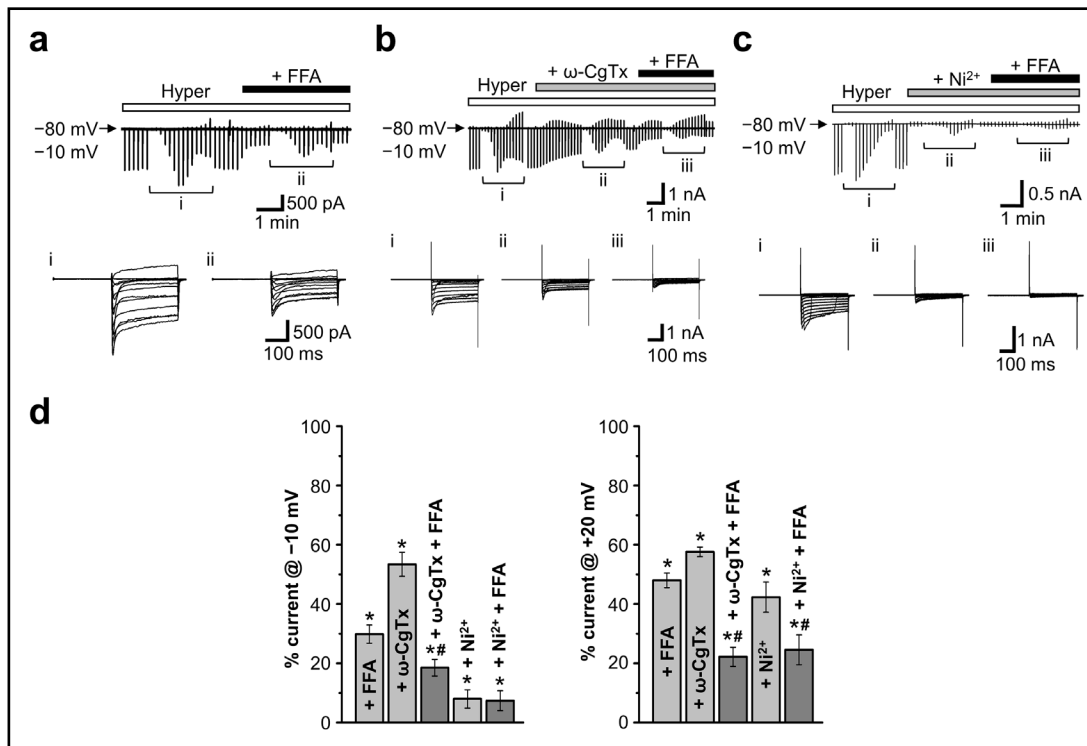


Fig. 6. The effects of FFA in the absence and presence of ω -CgTx or Ni^{2+} on VGCC currents under hyperosmotic conditions. (a) Representative record of currents before and after application of FFA under hyperosmotic conditions. Inset panels given below the current trace represent expanded current responses to step pulses from -60 to $+70$ mV applied at i and ii. (b, c) Representative records of currents before and after application of FFA in the absence and presence of $0.5 \mu\text{M}$ ω -CgTx (b) or 3 mM Ni^{2+} (c) under hyperosmotic conditions. Inset panels given below the current traces represent expanded traces of current responses to step pulses from -60 to $+70$ mV applied at i, ii and iii. (d) Percent currents observed at -10 mV (left panel) and $+20$ mV (right panel) in the presence of FFA, ω -CgTx, ω -CgTx plus FFA, Ni^{2+} , and Ni^{2+} plus FFA compared to the control currents (Control) in the absence of these blockers ($n=8-16$). * $p<0.05$ vs. Control. # $p<0.05$ vs. $+\omega$ -CgTx or $+Ni^{2+}$.

eGFP expression, and ω -CgTx-sensitive (mainly N-type) and Ni^{2+} -sensitive (mainly T-type) VGCC channels were found to be predominantly functioning in the plasma membrane of AVP neurons under hyperosmotic stimulation by whole-cell recordings (Fig. 5). Also, both N- and T-type Ca^{2+} channels in AVP neurons were found to be sensitive to FFA under hyperosmotic conditions (Fig. 6). In addition, the spontaneous firing in AVP neurons under hyperosmotic stimulation was virtually abolished by FFA and Ni^{2+} (Fig. 4), suggesting that the firing activity under acute hyperosmotic conditions is caused mainly by T-type VGCC channels.

The ability of cell volume regulation is fundamental to the survival and function of animal cells under not only physiological conditions but also pathological situations [1-4, 31, 63, 64]. The volume regulation processes are classified into RVD and RVI, that take place after cell swelling and shrinkage, respectively, and they are essentially involved not only in the relief of osmotic volume perturbation but also in cell shape changes associated with cell proliferation or mitosis, differentiation and migration [2, 55, 65, 66]. Persistent cell swelling and shrinkage lead to induction of necrotic and apoptotic cell death, respectively [4, 67]. On the other hand, rat SON MNCs were reported to exhibit sustained cell swelling and shrinkage in response to hypoosmotic and hyperosmotic stimulation, respectively, without showing discernible cell volume regulation [6]. However, we demonstrated that AVP neurons identified by transgenic eGFP expression can respond to a hypoosmotic challenge with a slow RVD event which is attained by activation of volume-sensitive outwardly rectifying anion channels (VSORs) by

osmotic cell swelling and AVP receptor-mediated autocrine signaling [7]. In the present study, eGFP-identified AVP neurons were found to respond with sustained cell shrinkage to a hyperosmotic challenge without apparently showing volume recovery (Fig. 1a). However, when FFA was added to a hyperosmotic solution, a typical RVI event became evident after osmotic cell shrinkage in the AVP neurons (Fig. 3a). The RVI event observed in the presence of FFA was completely eliminated by application of amiloride and DIDS (Fig. 3a, c) that are blockers of NHE and AE, respectively. In contrast, as shown in Fig. 1b, changes in the CSA values of AVP neurons after exposure to a hyperosmotic solution were affected neither by benzamil, which is known to block ENaC much more strongly than amiloride [34], nor by 3-AB, which is known to block PARP [35] and thereby suppress PARP-dependent TRPM2 channel activity [36]. Thus, NHE and AE are likely involved in the RVI process in the presence of FFA in AVP neurons. Taken together, it appears that rat AVP neurons do possess the RVI ability which is largely attained by parallel operation of NHE and AE, and that the RVI event is hidden behind some additional cell shrinkage process which is sensitive to FFA.

Essentially similar RVI-actualizing effects of FFA were found to be duplicated by application of a vesicular transport inhibitor, TeTx, and a known T-type VGCC blocker, Ni²⁺, in AVP neurons upon a hyperosmotic challenge (Fig. 3b, c). In addition, not only TeTx but also Ni²⁺ and FFA were found to prominently inhibit somatodendritic AVP secretion (Fig. 3d). Exocytotic AVP secretion from both axon terminals and somata/dendrites is known to be regulated by the frequency and pattern of action potential firings generated in the soma due to activation of both Na⁺ and Ca²⁺ channels [45, 68, 69]. In fact, firing activity in eGFP-identified AVP neurons was enhanced by hyperosmotic stimulation in a manner sensitive to Ni²⁺ and FFA (Fig. 4). Thus, an FFA-sensitive component of cell shrinkage represents an SVD event [20] which was observed in a number of secretory cells during stimulation with a variety of secretagogues [5, 20-27]. Taken together, it is concluded that the AVP neurons exhibit three different types of volume responses to a hyperosmotic challenge; that is, physical osmotic cell shrinkage as well as physiological SVD and RVI events.

Ni²⁺ is known to block a number of VGCCs [70], preferentially T-type Ca²⁺ channels [71, 72]. FFA was shown to inhibit L-type Ca²⁺ channels in rat smooth muscle cells [73]. Thus, a possibility arises that FFA blocks Ni²⁺-sensitive VGCCs in rat AVP neurons, with inhibiting hyperosmolarity-induced enhancement of firing activity and AVP secretion coupled to an SVD event. In the present study, actually, both Ni²⁺ and FFA were found to prominently suppress VGCC currents in AVP neurons under hyperosmotic stimulation (Fig. 5 and 6). Pharmacological experiments showed that hyperosmotic VGCC currents in AVP neurons are mainly composed of ω -CgTx-sensitive N-type and Ni²⁺-sensitive T-type Ca²⁺ channel currents (Fig. 5a, c) and that FFA could block both N- and T-type Ca²⁺ channel currents (Fig. 6b-d). Thus, it appears that rat AVP neurons respond to acute hyperosmotic stimulation not only with osmotic cell shrinkage but also with the SVD event due to massive somatodendritic AVP secretion that was triggered by activation of T-type Ca²⁺ channels, and that rat AVP neurons do exhibit the RVI event which is likely attained by parallel operation of NHE and AE coping with these dual volume decreasing events.

Accumulating evidence has shown that a number of important properties are different between AVP and OXT neurons [74]. Therefore, future studies are warranted to clarify whether OXT neurons distinguished from AVP neurons also respond to acute hyperosmotic stimulation not only with osmotic cell shrinkage but also with RVI and SVD events, and which types of VGCCs are activated upon a hyperosmotic challenge.

Conclusion

In summary, we revealed that AVP neurons retain the ability of RVI largely involving NHE and AE activities and also do exhibit the SVD response due to massive AVP exocytosis under hyperosmolar conditions. The volume recovery due to the RVI mechanism and the volume decrease due to the SVD event occurred in parallel in a manner approximately

cancelling out the volume changes of each other, and the volume recovery was therefore not apparently observed after the cell volume reduction by hyperosmotic stimulation. It is suggested that the SVD event was triggered by activation of Ni^{2+} - and FFA-sensitive voltage-gated Ca^{2+} channels in AVP neurons under hyperosmotic conditions.

Acknowledgements

Author Contributions

K.S.-N. conducted all experiments and data analysis. T.N. and Y.U. helped to design the work and commented on the draft. K.S.-N. and Y.O. conceived and designed the work and wrote the manuscript.

Funding Sources

This work was supported in part by Grants-in-Aid for Scientific Research (KAKENHI) from the Japan Society for the Promotion of Science (No. 18J40103) and by Grant of The Clinical Research Promotion Foundation (2020).

Statement of Ethics

All procedures performed in this study were in accordance with the regulations established at the Fukuoka University, with due consideration given to animal welfare and safety and health, and approved by the Ethics Committee of Animal Care and Experimentation, Fukuoka University, Japan (approval No.: 1906025).

Disclosure Statement

The authors have no conflicts of interest to declare.

References

- 1 Hoffmann EK, Lambert IH, Pedersen SF: Physiology of cell volume regulation in vertebrates. *Physiol Rev* 2009;89:193-277.
- 2 Lang F, Busch GL, Ritter M, Volkl H, Waldegger S, Gulbins E, Haussinger D: Functional significance of cell volume regulatory mechanisms. *Physiol Rev* 1998;78:247-306.
- 3 Okada Y: Cell volume regulation: the molecular mechanism and volume sensing machinery. Elsevier 1998:17-21.
- 4 Okada Y, Maeno E, Shimizu T, Manabe K, Mori S, Nabekura T: Dual roles of plasmalemmal chloride channels in induction of cell death. *Pflugers Arch* 2004;448:287-295.
- 5 Pedersen S, Hoffmann E, Novak I: Cell volume regulation in epithelial physiology and cancer. *Front Physiol* 2013;4:233.
- 6 Zhang Z, Bourque CW: Osmometry in osmosensory neurons. *Nat Neurosci* 2003;6:1021.
- 7 Sato K, Numata T, Saito T, Ueta Y, Okada Y: V_2 receptor-mediated autocrine role of somatodendritic release of AVP in rat vasopressin neurons under hypo-osmotic conditions. *Sci Signal* 2011;4:ra5.
- 8 Dayanithi G, Weller U, Ahnert-Hilger G, Link H, Nordmann JJ, Gratzl M: The light chain of tetanus toxin inhibits calcium-dependent vasopressin release from permeabilized nerve endings. *Neuroscience* 1992;46:489-493.
- 9 Ludwig M, Callahan MF, Neumann I, Landgraf R, Morris M: Systemic osmotic stimulation increases vasopressin and oxytocin release within the supraoptic nucleus. *J Neuroendocrinol* 1994;6:369-373.
- 10 Ludwig M, Horn T, Callahan MF, Grosche A, Morris M, Landgraf R: Osmotic stimulation of the supraoptic nucleus: central and peripheral vasopressin release and blood pressure. *Am J Physiol Endocrinol Metab* 1994;266:E351-E356.

- 11 Tobin VA, Ludwig M: The actin filament and dendritic peptide release. *Biochem Soc Trans* 2007;35:1243-1246.
- 12 Kombian SB, Mougnot D, Pittman QJ: Dendritically released peptides act as retrograde modulators of afferent excitation in the supraoptic nucleus *in vitro*. *Neuron* 1997;19:903-912.
- 13 Gouzènes L, Desarmenien MG, Hussy N, Richard P, Moos FC: Vasopressin regularizes the phasic firing pattern of rat hypothalamic magnocellular vasopressin neurons. *J Neurosci* 1998;18:1879-1885.
- 14 Alonso G, Gallibert E, Lafont C, Guillon G: Intrahypothalamic angiogenesis induced by osmotic stimuli correlates with local hypoxia: a potential role of confined vasoconstriction induced by dendritic secretion of vasopressin. *Endocrinology* 2008;149:4279-4288.
- 15 de Kock CP, Wierda KD, Bosman LW, Min R, Koksma JJ, Mansvelde HD, Verhage M, Brussaard AB: Somatodendritic secretion in oxytocin neurons is upregulated during the female reproductive cycle. *J Neurosci* 2003;23:2726-2734.
- 16 Cazalis M, Dayanithi G, Nordmann JJ: Hormone release from isolated nerve endings of the rat neurohypophysis. *J Physiol* 1987;390:55-70.
- 17 Di Scala-Guenot D, Strosser MT, Richard P: Electrical stimulations of perfused magnocellular nuclei *in vitro* elicit Ca^{2+} -dependent, tetrodotoxin-insensitive release of oxytocin and vasopressin. *Neurosci Lett* 1987;76:209-214.
- 18 Ludwig M, Sabatier N, Bull PM, Landgraf R, Dayanithi G, Leng G: Intracellular calcium stores regulate activity-dependent neuropeptide release from dendrites. *Nature* 2002;418:85-89.
- 19 Tobin V, Gouty LA, Moos FC, Desarmenien MG: A store-operated current (SOC) mediates oxytocin autocontrol in the developing rat hypothalamus. *Eur J Neurosci* 2006;24:400-404.
- 20 Manabe K, Shimizu T, Morishima S, Okada Y: Regulatory volume increase after secretory volume decrease in colonic epithelial cells under muscarinic stimulation. *Pflugers Arch* 2004;448:596-604.
- 21 Bachmann O, Heinzmann A, Mack A, Manns MP, Seidler U: Mechanisms of secretion-associated shrinkage and volume recovery in cultured rabbit parietal cells. *Am J Physiol Gastrointest Liver Physiol* 2007;292:G711-G717.
- 22 Dissing S, Hansen HJ, Undén M, Nauntofte B: Inhibitory effects of amitriptyline on the stimulation-induced Ca^{2+} increase in parotid acini. *Eur J Pharmacol* 1990;177:43-54.
- 23 Foskett JK: $[Ca^{2+}]_i$ modulation of Cl^- content controls cell volume in single salivary acinar cells during fluid secretion. *Am J Physiol Cell Physiol* 1990;259:C998-C1004.
- 24 Lee RJ, Foskett JK: Mechanisms of Ca^{2+} -stimulated fluid secretion by porcine bronchial submucosal gland serous acinar cells. *Am J Physiol Lung Cell Mol Physiol* 2010;298:L210-L231.
- 25 Nakahari T, Murakami M, Sasaki Y, Kataoka T, Imai Y, Shiba Y, Kanno Y: Dose effects of acetylcholine on the cell volume of rat mandibular salivary acini. *Jpn J Physiol* 1991;41:153-168.
- 26 Nakahari T, Murakami M, Yoshida H, Miyamoto M, Sohma Y, Imai Y: Decrease in rat submandibular acinar cell volume during ACh stimulation. *Am J Physiol Gastrointest Liver Physiol* 1990;258:G878-G886.
- 27 Numata T, Sato-Numata K, Okada Y, Inoue R: Cellular mechanism for herbal medicine Junchoto to facilitate intestinal Cl^- /water secretion that involves cAMP-dependent activation of CFTR. *J Nat Med* 2018;72:694-705.
- 28 Ueta Y, Fujihara H, Serino R, Dayanithi G, Ozawa H, Matsuda K, Kawata M, Yamada J, Ueno S, Fukuda A, Murphy D: Transgenic expression of enhanced green fluorescent protein enables direct visualization for physiological studies of vasopressin neurons and isolated nerve terminals of the rat. *Endocrinology* 2005;146:406-413.
- 29 Numata T, Sato K, Christmann J, Marx R, Mori Y, Okada Y, Wehner F: The deltaC splice-variant of TRPM2 is the hypertonicity-induced cation channel in HeLa cells, and the ecto-enzyme CD38 mediates its activation. *J Physiol* 2012;590:1121-1138.
- 30 Plettenberg S, Weiss EC, Lemor R, Wehner F: Subunits alpha, beta and gamma of the epithelial Na^+ channel (ENaC) are functionally related to the hypertonicity-induced cation channel (HICC) in rat hepatocytes. *Pflugers Arch* 2008;455:1089-1095.
- 31 Hoffmann EK, Simonsen LO: Membrane mechanisms in volume and pH regulation in vertebrate cells. *Physiol Rev* 1989;69:315-382.
- 32 Okada Y: Ion channels and transporters involved in cell volume regulation and sensor mechanisms. *Cell Biochem Biophys* 2004;41:233-258.

- 33 Wehner F, Tinel H: Role of Na⁺ conductance, Na⁺-H⁺ exchange, and Na⁺-K⁺-2Cl⁻ symport in the regulatory volume increase of rat hepatocytes. *J Physiol* 1998;506:127-142.
- 34 Kleyman TR, Cragoe EJ, Jr.: Amiloride and its analogs as tools in the study of ion transport. *J Membr Biol* 1988;105:1-21.
- 35 Purnell MR, Whish WJ: Novel inhibitors of poly (ADP-ribose) synthetase. *Biochem J* 1980;185:775-777.
- 36 Roberge S, Roussel J, Andersson DC, Meli AC, Vidal B, Blandel F, Lanner JT, Le Guennec JY, Katz A, Westerblad H, Lacampagne A, Fauconnier J: TNF- α -mediated caspase-8 activation induces ROS production and TRPM2 activation in adult ventricular myocytes. *Cardiovasc Res* 2014;103:90-99.
- 37 Sato-Numata K, Numata T, Ueta Y, Okada Y: Expression and functions of N-type Cav2.2 and T-type Cav3.1 channels in rat vasopressin neurons under normotonic conditions. *J Physiol Sci* 2020;70:49.
- 38 Fisher TE, Bourque CW: Calcium-channel subtypes in the somata and axon terminals of magnocellular neurosecretory cells. *Trends Neurosci* 1996;19:440-444.
- 39 Ortiz-Miranda SI, Dayanithi G, Velazquez-Marrero C, Custer EE, Treistman SN, Lemos JR: Differential modulation of N-type calcium channels by micro-opioid receptors in oxytocinergic versus vasopressinergic neurohypophysial terminals. *J Cell Physiol* 2010;225:276-288.
- 40 Wang D, Fisher TE: Expression of CaV 2.2 and splice variants of CaV 2.1 in oxytocin- and vasopressin-releasing supraoptic neurones. *J Neuroendocrinol* 2014;26:100-110.
- 41 Wang G, Dayanithi G, Kim S, Hom D, Nadasdi L, Kristipati R, Ramachandran J, Stuenkel EL, Nordmann JJ, Newcomb R, Lemos JR: Role of Q-type Ca²⁺ channels in vasopressin secretion from neurohypophysial terminals of the rat. *J Physiol* 1997;502:351-363.
- 42 Bicknell RJ: Optimizing release from peptide hormone secretory nerve terminals. *J Exp Biol* 1988;139:51-65.
- 43 Fisher TE, Bourque CW: The function of Ca²⁺ channel subtypes in exocytotic secretion: new perspectives from synaptic and non-synaptic release. *Prog Biophys Mol Biol* 2001;77:269-303.
- 44 Ludwig M, Bull PM, Tobin VA, Sabatier N, Landgraf R, Dayanithi G, Leng G: Regulation of activity-dependent dendritic vasopressin release from rat supraoptic neurones. *J Physiol* 2005;564:515-522.
- 45 Poulain DA, Wakerley JB: Electrophysiology of hypothalamic magnocellular neurones secreting oxytocin and vasopressin. *Neuroscience* 1982;7:773-808.
- 46 Sabatier N, Richard P, Dayanithi G: L-, N- and T- but neither P- nor Q-type Ca²⁺ channels control vasopressin-induced Ca²⁺ influx in magnocellular vasopressin neurones isolated from the rat supraoptic nucleus. *J Physiol* 1997;503:253-268.
- 47 Hussy N, Deleuze C, Desarménien MG, Moos FC: Osmotic regulation of neuronal activity: a new role for taurine and glial cells in a hypothalamic neuroendocrine structure. *Prog Neurobiol* 2000;62:113-134.
- 48 Moriya T, Shibasaki R, Kayano T, Takebuchi N, Ichimura M, Kitamura N, Asano A, Hosaka YZ, Forostyak O, Verkhatsky A, Dayanithi G, Shibuya I: Full-length transient receptor potential vanilloid 1 channels mediate calcium signals and possibly contribute to osmoreception in vasopressin neurones in the rat supraoptic nucleus. *Cell Calcium* 2015;57:25-37.
- 49 Sharif Naeini R, Witty MF, Seguela P, Bourque CW: An N-terminal variant of Trpv1 channel is required for osmosensory transduction. *Nat Neurosci* 2006;9:93-98.
- 50 Kasai H, Aosaki T, Fukuda J: Presynaptic Ca-antagonist omega-conotoxin irreversibly blocks N-type Ca-channels in chick sensory neurons. *Neurosci Res* 1987;4:228-235.
- 51 Plummer MR, Logothetis DE, Hess P: Elementary properties and pharmacological sensitivities of calcium channels in mammalian peripheral neurons. *Neuron* 1989;2:1453-1463.
- 52 Williams ME, Brust PF, Feldman DH, Patthi S, Simerson S, Maroufi A, McCue AF, Velicelebi G, Ellis SB, Harpold MM: Structure and functional expression of an omega-conotoxin-sensitive human N-type calcium channel. *Science* 1992;257:389-395.
- 53 Tobin VA, Douglas AJ, Leng G, Ludwig M: The involvement of voltage-operated calcium channels in somato-dendritic oxytocin release. *PLoS One* 2011;6:e25366.
- 54 Wang G, Dayanithi G, Newcomb R, Lemos JR: An R-type Ca²⁺ current in neurohypophysial terminals preferentially regulates oxytocin secretion. *J Neurosci* 1999;19:9235-9241.
- 55 Akita T, Okada Y: Characteristics and roles of the volume-sensitive outwardly rectifying (VSOR) anion channel in the central nervous system. *Neuroscience* 2014;275:211-231.
- 56 Fisher TE, Bourque CW: Voltage-gated calcium currents in the magnocellular neurosecretory cells of the rat supraoptic nucleus. *J Physiol* 1995;486:571-580.

- 57 Fisher TE, Bourque CW: Distinct omega-agatoxin-sensitive calcium currents in somata and axon terminals of rat supraoptic neurones. *J Physiol* 1995;489:383-388.
- 58 Foehring RC, Armstrong WE: Pharmacological dissection of high-voltage-activated Ca²⁺ current types in acutely dissociated rat supraoptic magnocellular neurons. *J Neurophysiol* 1996;76:977-983.
- 59 Joux N, Chevalerey V, Alonso G, Boissin-Agasse L, Moos FC, Desarménien MG, Hussy N: High voltage-activated Ca²⁺ currents in rat supraoptic neurones: biophysical properties and expression of the various channel alpha1 subunits. *J Neuroendocrinol* 2001;13:638-649.
- 60 Shibuya I, Noguchi J, Tanaka K, Harayama N, Inoue Y, Kabashima N, Ueta Y, Hattori Y, Yamashita H: PACAP increases the cytosolic Ca²⁺ concentration and stimulates somatodendritic vasopressin release in rat supraoptic neurons. *J Neuroendocrinol* 1998;10:31-42.
- 61 Zhang W, Star B, Rajapaksha WRAKJS, Fisher TE: Dehydration increases L-type Ca²⁺ current in rat supraoptic neurons. *J Physiol Sci* 2007;580:181-193.
- 62 Erickson KR, Ronnekleiv OK, Kelly MJ: Role of a T-type calcium current in supporting a depolarizing potential, damped oscillations, and phasic firing in vasopressinergic guinea pig supraoptic neurons. *Neuroendocrinology* 1993;57:789-800.
- 63 Delpire E, Gagnon KB: Water homeostasis and cell volume maintenance and regulation. *Curr Top Membr* 2018;81:3-52.
- 64 Okada Y: Channelling frozen cells to survival after thawing: opening the door to cryo-physiology. *J Physiol* 2016;594:1523-1524.
- 65 Okada Y: Volume expansion-sensing outward-rectifier Cl⁻ channel: fresh start to the molecular identity and volume sensor. *Am J Physiol Cell Physiol* 1997;273:C755-C789.
- 66 Wehner F, Olsen H, Tinel H, Kinne-Saffran E, Kinne RK: Cell volume regulation: osmolytes, osmolyte transport, and signal transduction. *Rev Physiol Biochem Pharmacol* 2003;148:1-80.
- 67 Okada Y, Maeno E, Shimizu T, Dezaki K, Wang J, Morishima S: Receptor-mediated control of regulatory volume decrease (RVD) and apoptotic volume decrease (AVD). *J Physiol* 2001;532:3-16.
- 68 Bourque CW, Renaud LP: Calcium-dependent action potentials in rat supraoptic neurosecretory neurones recorded *in vitro*. *J Physiol* 1985;363:419-428.
- 69 Mason WT, Leng G: Complex action potential waveform recorded from supraoptic and paraventricular neurones of the rat: evidence for sodium and calcium spike components at different membrane sites. *Exp Brain Res* 1984;56:135-143.
- 70 Zamponi GW, Bourinet E, Snutch TP: Nickel block of a family of neuronal calcium channels: subtype- and subunit-dependent action at multiple sites. *J Membr Biol* 1996;151:77-90.
- 71 Lee JH, Gomora JC, Cribbs LL, Perez-Reyes E: Nickel block of three cloned T-type calcium channels: low concentrations selectively block alpha1H. *Biophys J* 1999;77:3034-3042.
- 72 Obejero-Paz CA, Gray IP, Jones SW: Ni²⁺ block of CaV3.1 (alpha1G) T-type calcium channels. *J Gen Physiol* 2008;132:239-250.
- 73 Shimamura K, Zhou M, Ito Y, Kimura S, Zou LB, Sekiguchi F, Kitamura K, Sunano S: Effects of flufenamic acid on smooth muscle of the carotid artery isolated from spontaneously hypertensive rats. *J Smooth Muscle Res* 2002;38:39-50.
- 74 Armstrong WE, Foehring RC, Kirchner MK, Sladek CD: Electrophysiological properties of identified oxytocin and vasopressin neurones. *J Neuroendocrinol* 2019;31:e12666.